The mammalian Ire1 inhibitor, 4μ8C, exhibits broad anti-*Aspergillus* activity *in vitro* and in a treatment model of fungal keratitis.

Manali M. Kamath[1*], Emily M. Adams[2], Jorge D. Lightfoot[2], Becca L. Wells[1], and Kevin K. Fuller[1,2*†]

1 Department of Microbiology & Immunology, University of Oklahoma Health Sciences Center, Oklahoma City, OK

2 Department of Ophthalmology, University of Oklahoma Health Sciences Center, Oklahoma City, OK

* **Current Address**:   Department of Ophthalmology

University of Pittsburgh School of Medicine

1622 Locust St., Pittsburgh, PA, 15219

†Correspondence: Kevin K. Fuller, Ph.D.

Associate Professor, Department of Ophthalmology

University of Pittsburgh School of Medicine

Email: kkf18@pitt.edu

Phone: 412-648-7707

22   **Abstract**

23   **Objective:** The fungal unfolded protein response consists of a two-component relay in which the
24   ER-bound sensor, IreA, splices and activates the mRNA of the transcription factor, HacA.
25   Previously, we demonstrated that *hacA* is essential for *Aspergillus fumigatus* virulence in a murine
26   model of fungal keratitis (FK), suggesting the pathway could serve as a therapeutic target. Here
27   we investigate the antifungal properties of known inhibitors of the mammalian Ire1 protein both *in*
28   *vitro* and in a treatment model of FK.

29   **Methods:** The antifungal activity of Ire1 inhibitors was tested against conidia of several *A.*
30   *fumigatus* isolates by a microbroth dilution assay and against fungal biofilm by XTT reduction.
31   The influence of 4µ8C on *hacA* mRNA splicing in *A. fumigatus* was assessed through gel
32   electrophoresis and qRT-PCR of UPR regulatory genes. The toxicity and antifungal profile of
33   4µ8C in the cornea was assessed by applying drops to uninfected or *A. fumigatus*-infected
34   corneas 3 times daily starting 4 hours post-inoculation. Corneas were evaluated daily through slit-
35   lamp imaging and optical coherence tomography, or at endpoint through histology or fungal
36   burden quantification via colony forming units.

37   **Results:** Among six Ire1 inhibitors screened, the endonuclease inhibitor 4µ8C displayed the
38   strongest antifungal profile with an apparent fungicidal action. The compound both blocked
39   conidial germination and hyphal metabolism of *A. fumigatus* Af293 in the same concentration
40   range that blocked *hacA* splicing and UPR gene induction (60-120 µM). Topical treatment of
41   sham-inoculated corneas with 0.5 and 2.5 mM 4µ8C did not impact corneal clarity, but did
42   transiently inhibit epithelialization of corneal ulcers. Relative to vehicle-treated Af293-infected
43   corneas, treatment with 0.5 and 2.5 mM drug resulted in a 50% and >90% reduction in fungal
44   load, respectively, the latter of which corresponded to an absence of clinical signs of infection or
45   corneal pathology.

46   **Conclusion:** The *in vitro* data suggest that 4µ8C displays antifungal activity against *A. fumigatus*
47   through the specific inhibition of IreA. Topical application of the compound to the murine cornea
48   can furthermore block the establishment of infection, suggesting this class of drugs can be
49   developed as novel antifungals that improve visual outcomes in FK patients.

50

51   **KEYWORDS:** Fungal keratitis, IRE1 inhibitors, 4µ8C, *Aspergillus fumigatus*, antifungals.

52

1 Introduction

Fungal infections of the cornea are an ophthalmologic emergency and represent a leading cause of ocular morbidity and unilateral blindness worldwide (1,2). This disease entity, called fungal keratitis (FK), typically affects otherwise healthy individuals that are inoculated with fungal spores or hyphae through ocular trauma or contact lens wear (3,4). Even with the current standard of treatment, which includes topical application of natamycin or voriconazole, 40-60% of all FK cases result in corneal perforation and/or the need for corneal transplantation (5,6). One approach to the development of novel antifungals for FK, or indeed any clinical context, is a biologically-informed one that involves two key steps: first, the identification of a fungal protein/pathway that is essential for growth or virulence in a relevant disease model and, second, identification of a small molecule(s) that inhibits protein function and improves disease outcome in the model without toxicity to the host. In the context of this study, we and others have previously identified the unfolded protein response (UPR) as a critical regulator of *Aspergillus fumigatus* virulence in both lung and cornea infection models, and now seek to develop inhibitors of the pathway as novel antifungals (7–9).

The mammalian UPR consists of three separate but partially redundant signaling branches – IRE1, ATF6, and PERK - where the Ire1 branch is the most highly conserved across the eukaryotes and is the only one found in the fungi (10–14). In *A. fumigatus*, the Ire1 ortholog (IreA) is an ER-bound transmembrane protein comprised of a luminal sensory domain and two cytosolic domains that propagate the signal to the nucleus (7,15). More completely, the rapid accumulation of misfolded proteins in the ER lumen promotes the oligomerization of IreA within the membrane. This clustering triggers the trans-autophosphorylation of the kinase domain and subsequent activation of the endoribonuclease domain which then splices an unconventional intron from its only known client mRNA, *hacA*. The spliced *hacA* isoform encodes a bZIP transcription factor, HacA, which regulates genes not only involved directly in protein folding homeostasis (e.g. chaperones and foldases), but also genes involved in primary and secondary metabolism that altogether promote adaptation to stressful environments (7,9,16,17). Recently, we demonstrated that a *hacA* deletion mutant of *A. fumigatus* (Af293 background) is viable under normal growth conditions but is unable to establish infection in a murine model of fungal keratitis (9). Surprisingly, we were unable to isolate an *ireA* deletant in Af293 and repression of the gene using a tetracycline regulatable promoter blocks hyphal growth (9). Not only does this indicate that IreA regulates fungal growth beyond its influence of HacA, but it pragmatically suggests the protein could serve as an ideal target for antifungal intervention.

Several small molecules are known to inhibit the mammalian Ire1 kinase or endonuclease domains and, consistent with the UPR's role in regulating cellular homeostasis, display anti-proliferative effects various cell culture or *in vivo* cancer models, including those related to hepatocellular carcinoma, acute myeloid leukemia, triple negative breast cancer, and multiple myeloma (15-21). Recently, Guirao-Abad and colleagues demonstrated that one such compound, the coumarin derivative 4-methyl umbilliferone 8-carbaldehyde (4µ8C), inhibits the endonuclease activity of *A. fumigatus* IreA and consequently the downstream expression of canonical HacA-dependent genes in the setting of acute ER stress (18). The utility of 4µ8C or other Ire1 inhibitors as clinically useful antifungals, however, has not been explored. In this study, we assess the intrinsic antifungal activity of six Ire1 compounds against common laboratory and corneal isolates of *A. fumigatus,* as well as the ability of the most broadly active compound, 4µ8C, to influence disease outcomes in a murine model of FK.

2 Materials and Methods

2.1 Chemical reagents used in the study. All IRE1 inhibitors were prepared in dimethyl sulfoxide (DMSO) and stored at -80 °C until use. 50 mM stock of IRE1 inhibitor III, 4µ8C (#412512 - MilliporeSigma, MA, USA), 50 mM Sunitinib (HY-10255A – MedChemExpress, NJ, USA), 10 mM Z4P (HY-153773 – MedChemExpress, NJ, USA), 10 mM STF-083010 (HY-15845 –

3

104   MedChemExpress, NJ, USA), 10 mM KIRA6 (HY-19708 – MedChemExpress, NJ, USA) and 10
105   mM HY-114368 (HY-15845 – MedChemExpress, NJ, USA) were used. DL-Dithiothreitol (#0281
106   DTT- VWR, PA, USA) was prepared at 1 M concentration in sterile PBS.
107
108   **2.2 Strains and growth conditions.** The FK1 and FK2 *A. fumigatus* isolates are from fungal
109   keratitis patients at the University of California at San Francisco-Proctor Foundation. An Af293
110   derivative strain that constitutively expresses the *mcherry* protein (Af293::*PgpdA-mcherry-hph*)
111   was used throughout this study (9,19). Strains were maintained on glucose minimal media (GMM)
112   containing 1% glucose, Clutterbuck salts, and Hutner's trace elements, 10 mM ammonium tartrate
113   (GMM) at pH 6.5 (20). To test the effect of the IRE1 inhibitors on the different *Aspergillus* strains,
114   10^6 conidia/mL were inoculated in GMM at a concentration gradient (0 - 480 μM) and incubated
115   at 35 °C. After 72 h, minimum inhibitory concentration (MIC) was recorded by visually inspecting
116   the plate and looking for the growth of the fungi under the microscope. To assess the fungicidal
117   effect of the IRE1 inhibitors, 10^6 conidia/mL were inoculated in GMM with either 4μ8C or STF-
118   083010 at a concentration gradient (0 - 480 μM) and incubated at 35 °C. 100 μL aliquots were
119   plated on YPD after 72 h in triplicate. These plates were incubated at 35 °C for 24 h to count the
120   number of colony-forming units (CFU). To quantify fungal growth, the XTT metabolic assay was
121   performed as described previously (21). XTT buffer was prepared at a stock of 0.5 mg/mL and
122   menadione at 10 mM in 100% acetone (final conc. 1 μM). For this assay, 10^6 conidia/mL were
123   inoculated in GMM in 96-well plate and incubated at 35 °C for 24h to form hyphae followed by
124   treatment with 4μ8C (0 – 240 μM) for 2h. Next, 100 μL of an XTT-menadione mixture was added
125   to each test well and incubated further for 2 h at 35 °C. Supernatants from each well (75 μL) were
126   assayed at 490 nm.
127
128   **2.3 RT-PCR analyses.** Fungal cultures were grown overnight at 35 °C in GMM in 6-well plates
129   were treated with a concentration gradient of 4μ8C (0 – 120 μM) for 2 h followed by treatment
130   with 10 mM DTT or vehicle for 2 h. RNA was then extracted from these cultures using RNeasy
131   Mini kit (#74106 Qiagen, Germany) followed by DNase treatment using the DNase I kit (Millipore
132   Sigma, Massachusetts, USA). The Nanodrop 2000 (Thermo Fisher Scientific, Massachusetts,
133   USA) was used to assess the quantity and quality of the RNA. Subsequently, the RNA was
134   standardized for cDNA conversion utilizing the ProtoScript II First Strand cDNA Synthesis Kit (New
135   England Biolabs, Massachusetts, USA) following the provided protocol. To visualize *hacA*
136   splicing, the coding sequencing (spanning the predicted 20 bp unconventional intron) was
137   amplified and resolved by electrophoresis (3% agarose gel at 40 V for 10 h) as previously
138   described (9). For qRT-PCR analysis, Luna Universal qPCR master mix (SYBR green; NEB, USA)
139   was used on the QuantStudio 3 Real-Time PCR System (Thermo Fisher Scientific,
140   Massachusetts, USA), and the analysis was conducted with QuantStudio Design and Analysis
141   Software v1.5.2. Fold-expression changes were computed using the 2-ΔΔCt method, followed by
142   analysis using MS-Excel. The primers used to amplify *hacA*, *bipA* and *pdiA* in this assay are the
143   same as previously published (9,18).
144
145   **2.4 Animals**
146   Inoculum: $5x10^6$ conidia were incubated in 20 ml YPD at 35 °C for approximately 4 h until mostly
147   swollen. Biomass was collected, washed 4x with PBS, and resuspended in 500 μL PBS, adjusting
148   volumes to normalize strains to 0.8 at OD 360 nm. Infections: 6-8-week-old C57B6/6J (Jackson
149   Laboratory) received intraperitoneal immunosuppression with 100 mg/kg Depo-Medrol (Zoetis,
150   USA) on day -1. On day 0, mice were anesthetized using 100 mg/kg ketamine and 6.6 mg/kg
151   xylazine by IP injection, and their right eyes abraded to a 1 mm diameter using Algerbrush II.
152   Fungal inocula (5 μL) were applied to ulcerated eyes and wiped with a kim wipe after 20 minutes.
153   The mice also received Buprenorphine SR (1 mg/kg) which was administered subcutaneously.
154   Contralateral eyes remained uninfected per ARVO guidelines. For controls, we used algerbrushed

155   sham-infected and untouched eyes. *Micron IV* slit-lamp (Phoenix Research Labs Inc., CA, USA)
156   was used to monitor mice daily post-inoculation (p.i.) up to 72 h. This procedure was performed
157   while the mice were anesthetized with isoflurane. *Anterior segment spectral-domain optical*
158   *coherent tomography* (OCT) measured corneal thickness at 48 and 72 h p.i. using a 4x4 mm
159   image using 12 mm telecentric lens from Leica Microsystems (IL, USA). The reference arm was
160   set to 885 according to the manufacturer's calibration instruction. Image analysis was conducted
161   using the InVivoVue diver software. Corneal thickness quantification involved measuring an 11x11
162   spider plot covering the entire eye, and an average of 13 readings were obtained. *Fluorescein*
163   *imaging:* Corneal fluorescein staining was performed to test the rate of healing of the abraded
164   epithelium post treatment with DMSO or 4µ8C. AK-Fluor 10% fluorescein solution (Akorn, IL,
165   USA) diluted 1:100 was applied to the corneas in isoflurane-anesthetized mice using a cotton
166   swab and excess was wiped off and imaged using a slit-lamp Micron (Phoenix Research Labs
167   Inc., CA, USA). *Histopathological analysis*: Control eyes were harvested after 72h and fixed with
168   10% neutral buffered formalin for 24 h followed by 70% ethanol until they were further processed.
169   5 µm thick sections of the eyes were stained with Hematoxylin and eosin (H&E) to evaluate host
170   inflammatory response after treatment with DMSO or 4µ8C. *Fungal burden determination:*
171   Corneas were dissected in a sterile manner, homogenized using a collagenase buffer at a
172   concentration of 2 mg/ml, and then 100 µl aliquots were plated in triplicate on inhibitory mold agar
173   (IMA) plates. The number of colony-forming units (CFU) per cornea was assessed after 24 hours
174   of incubation at 35°C. *Clinical scoring:* Micron images were randomized and scored (0 to 4 scale)
175   for clinical pathology by reviewers not involved with the experiment based on previously
176   established criteria, including surface regularity, area of opacification, and density of opacification
177   (22). *Topical Treatments*: For the topical treatments of sham or Af293-inoculated corneas, animals
178   were anesthetized isoflurane and a 5 µL drop of the compound (or DMSO as a vehicle control)
179   was applied to the ocular surface. The animals were kept under anesthesia for 10 minutes with
180   the drop in place before being returned to their cage. The treatment schedule varied slightly
181   across experiments (see the corresponding figure legends), but generally consisted of one
182   treatment on the day of inoculation (4 h p.i.), three treatments (4 h apart) at 1 and 2 days p.i., and
183   one treatment at 3 days p.i., just prior to imaging and removal of the eyes for histological or fungal
184   burden analysis. In the case of the fluorescein experiments, the animals received three treatments
185   3 days p.i..

187   **2.5 Statistical analyses** were performed using GraphPad Prism 10 version 10.2.0. The specific
188   tests used for each experiment are described in the corresponding figure legends.

190   **3 Results**
191   **3.1 Ire1 endonuclease inhibitors display antifungal activity against *Aspergillus fumigatus***
192   **laboratory strains and clinical isolates.**
193   We first predicted that Ire1 inhibitors would display *in vitro* antifungal activity against Af293 and
194   potentially other *A. fumigatus* strains in which IreA influences fungal growth and or viability. We
195   began by screening the activity of six commercially available Ire1 inhibitors—including four kinase
196   domain inhibitors (sunitinib, Z4P, KIRA6, KIRA8) and two endonuclease domain inhibitors (4µ8C,
197   STF083010) (**Supplementary Figure 1**) in a microtiter dilution assay. Four *A. fumigatus* strains
198   were tested in the screen, including the well-studied Af293 and CEA10 strains (both pulmonary
199   isolates) and two uncharacterized corneal isolates from fungal keratitis patients, designated here
200   as FK1 and FK2. No inhibitory activity was observed with any of the four kinase inhibitors even at
201   the highest tested concentration (**Supplementary Figure 2**), suggesting that these compounds
202   either do not adequately accumulate within the fungal cell, they do not have high affinity for the
203   *A. fumigatus* kinase domain, or the domain itself is not essential for *A. fumigatus* growth in these
204   isolates. By contrast, both endonuclease inhibitors fully blocked conidial germination, with the two
205   exhibiting comparable minimal inhibitory concentrations (MICs) against the Af293 strain and 4µ8C

206 displaying overall lower MICs against the other three (**Table 1**). To gain some insight into whether
207 the inhibitory action of these compounds was fungistatic or fungicidal, the microtiter assay was
208 repeated with Af293 and, following 72 h incubation, media from the wells was sub-cultured onto
209 drug-free nutrient agar plates (**Figure 1A**). Samples corresponding to STF083010 inhibition (60-
210 480 µM) all yielded fungal colonies, suggesting the conidia were still viable and the drug is
211 fungistatic. All sub-culture corresponding to 4µ8C inhibition (120-480 µM), by contrast, remained
212 sterile, suggesting the drug may be fungicidal against the conidia (**Figure 1B**). To determine if
213 4µ8C can similarly affect fungal hyphae (i.e. the tissue invasive form), an XTT reduction assay
214 was performed on mycelia/biofilms cultured overnight in static culture and subsequently treated
215 with the drug for 2 h. As shown in **Figure 1C**, the 120 and 240 µM treatments resulted in a
216 markedly reduced or undetectable metabolic activity, respectively, altogether indicating that a
217 similar concentration of drug is fungicidal against both conidial and hyphal form of the organism.
218 Since 4µ8C provided the best antifungal profile, both in terms of its MIC and apparent fungicidal
219 action, we decided to prioritize that compound for downstream characterization.
220

	Af293	**CEA10**	**FK1**	**FK2**
4u8C	100 ±22.628	120 ±0.0	160 ±64.012	160 ±64.012
STF 083010	80 ±32.006	240 ±0.0	240 ±0.0	400 ±128.024

221

222 **Table 1:** Minimum inhibitory concentrations (MIC) for 4µ8C and STF 083010 against different *A.*
223 *fumigatus* isolates. Data reflect a mean (± SD) of 3 separate experimental runs, except for the
224 4µ8C/Af293 condition which was performed across 6 runs.

3.2 The antifungal activity of 4µ8C corresponds to an inhibition of Ire1 activity in Af293.

226 In biochemical assays, 4µ8C forms a Schiff base with distinct lysine residues in both the Ire1
227 kinase and endonuclease domains, but only inhibits the activity of the latter in treated cells (23).
228 This lysine is conserved in the *A. fumigatus* IreA endocnuclease domain, as is the influence of
229 the drug on *hacA* splicing in the AfS28/D141 background (18). We reasoned that if the antifungal
230 action of 4µ8C against Af293 were attributable to an 'on-target' effect, then there would be a
231 correspondence between the fungicidal MIC (ranging from 60 to 120 µM) and the inhibition of IreA
232 function. To explore this, fungal mycelia/biofilms were developed in GMM static culture overnight,
233 subsequently pretreated with DMSO (vehicle) or various concentrations of 4µ8C for 2 h, and
234 finally stimulated with 10 mM DTT for an additional 2 h. Samples treated with neither 4µ8C nor
235 DTT served as a control. The splicing status of *hacA* was then assessed by RT-PCR and gel
236 electrophoresis as previously described (9). As expected, treatment with DTT alone resulted in
237 an observable accumulation of the spliced/induced *hacA* product (*hacA*[i]), relative to untreated
238 controls, and the inclusion of 30 µM 4µ8C did not have an impact on this response. By contrast,
239 the *hacA*[i] splice form was completely absent in both the 60 and 120 µM 4µ8C treated samples,
240 thus establishing a putative connection between IreA function and fungal cell metabolism or
241 viability (**Figure 2A**). Sequencing of these end-point PCR products revealed that the canonical
242 (spliceosomal) intron at the 5' end of the *hacA* mRNA was absent in all samples, whereas the 20
243 bp IreA-targeted (non-canonical) intron was absent only in the DTT-treated fungus in the absence
244 of 4µ8C (**Figures 2C and 2D, Supplemental Figure 3**). Finally, in addition to a block in *hacA*
245 splicing, we further observed that 60 µM blocked the DTT-mediated induction *hacA* message as
246 well as two known HacA-regulated transcription factors, BipA and PdiA (**Figure 2B**). Taken
247 together, these results support a model in which 4µ8C blocks UPR signaling in *A. fumigatus,* and

6

248   by extension fungal metabolism and growth, through a specific action on IreA endonuclease
249   activity, rather than a broad inhibition of mRNA processing by the spliceosome.
250
251   **3.3 High dose 4μ8C treatment does not impact corneal clarity but does transiently inhibit**
252   **re-epithelialization.**
253   We were next interested in exploring the *in vivo* antifungal activity of 4μ8C in a murine model of
254   FK, but first had to consider the concentration to test. Ophthalmic antifungal formulations tend to
255   be highly concentrated to facilitate sufficient accumulation of the drug within the dense collagen
256   matrix of the cornea, particularly in the face of rapid dilution and drainage of the drug at the ocular
257   surface. For example, the *in vitro* MIC for natamycin against most *Aspergillus* isolates ranges
258   between 2-32 μg/mL, but is administered at 1, 500-25,000X this concentration in the form of hourly
259   50 mg/mL (75 mM) drops. Similarly, voriconazole drops are often formulated at 1 mg/mL (28 mM),
260   where the *in vitro* MIC for most *A. fumigatus* isolates is 0.25-4 μg/mL. Thus, while testing the
261   highest concentration of 4μ8C that its solubility permits (132.24 mM) would be desirable, we had
262   to further consider that the impact of the drug on corneal tissue homeostasis has not been
263   explored. We therefore began by testing the ocular toxicity profiles of two relatively conservative
264   4μ8C concentrations, 0.5 and 2.5 mM, which correspond to approximately 5X and 40X the *in vitro*
265   antifungal MIC, respectively.
266   The two drug concentrations were evaluated in sham model of FK previously developed
267   by our group, which involves the generation of an epithelial ulcer ahead of fungal inoculation, or
268   in this case, ulceration without the addition of fungus (9, 19). Each treatment consisted of a 5 μL
269   drop of 4μ8C or vehicle (DMSO) applied to the corneal surface up to three times daily per the
270   schedule described on the corresponding figure legends and methods. Corneas were tracked
271   daily by slit-lamp imaging to assess corneal clarity and ocular surface regularity, as well as by
272   optical coherence tomography (OCT) to measure corneal thickness and assess gross
273   morphology. Corneas were then resected at 72 h post-ulceration for histological analysis with
274   H&E staining. Relative to the vehicle control group, neither 4μ8C concentration had an observable
275   impact on corneal clarity or corneal thickness, suggesting the drug did not lead to acute
276   inflammation or edema (**Figure 3A, B** and **Supplementary Figures 4A, 4B**). Interestingly,
277   histology revealed that whereas the epithelium of vehicle-treated corneas had reformed, those
278   treated with either concentration of 4μ8C still appeared ulcerated (**Figure 3C** and **Supplementary**
279   **Figure 4C**). To evaluate this further, we replicated the experiment and followed reepithelization
280   (wound healing) longitudinally with fluorescein staining. Briefly, an intact corneal epithelium
281   precludes the entry of the stain into the underlying tissue, thus giving a negative signal on
282   fluorescence slit-lamp imaging; by contrast, ulcerated eyes give rise to diffuse yellow-green
283   staining of the stromal layer. As opposed to the vehicle-treated eyes, which fully precluded the
284   stain within 24 h post-ulceration, the 4μ8C-treated group remained positive for the duration of the
285   72 h treatment. We observed, however, that the corneas were fully healed within 3 days of
286   stopping treatment, suggesting that the drug has only a transient impact on epithelial cell
287   proliferation (**Figure 3D** and **Supplementary Figure 4D**). Taken together, we concluded that
288   tested treatment regimens of 4μ8C were minimally toxic to the murine cornea and suitable for
289   evaluation in a treatment model of FK.
290
291   **3.4 Topical treatment with 4μ8C blocks fungal growth and disease establishment in a**
292   **murine model of FK.**
293   To test the impact of 4μ8C on fungal growth and disease outcomes during FK, we inoculated
294   ulcerated corneas with swollen conidia of *A. fumigatus* Af293 (day 0) and treated on the same
295   schedule as described above—once on the day of ulceration/inoculation, three times at 24 and 48
296   h p.i,, and once at 72 h p.i.. Corneal disease metrics were tracked longitudinally by slit-lamp and
297   OCT as before, but included fungal burden assessment at 72 h by homogenizing and plating
298   corneas for colony forming unit (CFUs) measurement. We began with the 0.5 mM 4μ8C

299 preparation, where the lack of corneal toxicity on sham/uninfected corneas observed in the
300 previous safety trial was recapitulated. Furthermore, treatment at this concentration resulted in an
301 approximately 50% reduction in fungal load at 3 days p.i. relative to vehicle-treated FK corneas
302 (**Supplementary Figure 5A**). This reduction in fungal load did not, however, correspond to
303 improved clinical disease scores or reduced corneal thickness at any of the evaluated time points
304 (**Supplementary Figures 5B-D**), suggesting this treatment regimen is insufficient to block corneal
305 inflammation and tissue damage associated with FK pathology. We next tested the higher (2.5
306 mM) concentration of 4μ8C in the same manner and observed a >90% reduction in fungal burden
307 at 72 h p.i. that corresponded to an absence of corneal surface disease or cornea swelling at all
308 evaluated time points (**Figure 4**). These results suggested that the higher 4μ8C dosage led to a
309 rapid corneal sterilization that blocked the establishment of infection and downstream pathology.
310 The relative influence of 0.5 and 2.5 mM 4μ8C on fungal load and disease development was
311 recapitulated across multiple experiments with each concentration.
312
313 **4 Discussion**
314 The conservation of essential proteins between fungi and mammals is an important barrier to the
315 development of potent antifungals with acceptable host toxicity profiles. On the other hand,
316 existing drugs developed against human proteins, particularly those in the cancer therapeutic
317 pipeline, may display dually useful antifungal properties (24). In this report, we demonstrate that
318 the mammalian Ire1 inhibitor 4μ8C, which blocks tumor growth in various pre-clinical models,
319 inhibits the growth of various *A. fumigatus* isolates and can furthermore block the development of
320 fungal keratitis when applied topically to the corneal surface (25–27). These results underscore
321 the utility of drug repurposing efforts in the battle against medically important fungi, as well as the
322 importance of fungal keratitis as an important experimental platform towards this end.
323   Our interest in developing Ire1 inhibitors as antifungals was prompted by work in *A.
324 fumigatus* strain Af293, in which an *ireA* deletant could not be isolated and repression of the gene
325 via a regulatable promoter halted growth under standard laboratory conditions (9). Here we
326 demonstrate that 4μ8C fully blocks Af293 germination or hyphal metabolic activity at 60-120 μM,
327 which aligns closely with the drug concentration that inhibits IreA endonuclease activity. Thus, the
328 genetic and pharmacological data are seemingly in agreement and indicate that the antifungal
329 actiivty of 4μ8C is owed to the "on-target" inhibition of an essential *A. fumigatus* protein: IreA. The
330 possibility of "off-target" effects for 4μ8C, however, cannot be ruled out and may indeed be
331 implicated by two lines of evidence. First, we report here that STF-083010 displays a transient
332 inhibition of conidial germination against Af293 conidia, compared to the apparent fungicidal
333 action of 4μ8C, despite the two compounds ostensibly targeting the same lysine residue in the
334 IreA endonuclease domain (23). Second, work by others has established that *ireA* is not an
335 essential gene in a D141 derivative strain (AfS28) of *A. fumigatus*, yet 4μ8C can nevertheless
336 inhibit hyphal metabolism/viability of this strain at concentrations above which block IreA activity
337 (8,18). Thus, while it is possible that 4μ8C inhibits other essential enzymes or metabolic
338 processes that contribute to its *in vitro* antifungal activity, it is also likely that the exact influence
339 of the drug is variable across *A. fumigatus* lineages/isolates. We postulate that some *A. fumigatus*
340 lineages, such as Af293, experience a relatively higher level of ER stress during normal growth
341 that renders IreA essential and, by extension, 4μ8C fungicidal. Alternatively, other lineages such
342 as D141 may have recruited alternative signaling pathways that can compensate for IreA loss; in
343 these isolates, 4μ8C would only moderately impact growth *in vitro* until higher (i.e. off-target
344 inducing) concentrations of drug are applied. Such strain heterogeneity with respect to IreA
345 signaling is an ongoing line of investigation in our group. Nevertheless, *ireA* is essential for the
346 virulence of the D141 strain in the setting of invasive pulmonary aspergillosis (8), supporting its
347 feasibilty as an antifungal target irrespective of fungal background.
348   We demonstrate here that topical application of 2.5 mM 4μ8C (~40x the *in vitro* MIC in
349 GMM) to *A. fumigatus*-infected corneas can block fungal growth and the subsequent development

8

350 of disease. This effect is dose-dependent as treatment with less concentrated drops (0.5 mM)
351 results in only a 50% reduction in fungal burden and no discernable impact on the rate of disease
352 progression or severity. We believe these findings reflects a non-linear relationship between
353 fungal load in the cornea and clinical pathology, such that 1) a 50% reduction in fungal antigen
354 does not lead to a proportional reduction in the corneal inflammation and opacification or, 2) a
355 50% reduction in corneal inflammation is simply not clinically appreciable. Moreover, it is
356 furthermore unclear why the 0.5 mM concentration displays incomplete antifungal activity, despite
357 being 8X the *in vitro* MIC. We hypothesize that a combination of physical barriers, such has rapid
358 drainage from and slow tissue pentration through the cornea, act in concert with a fungal biological
359 response, such as drug efflux, to ultimately reduce the intracellular concentration of drug with the
360 fungal cell. Nevertheless, the fact that an effective antifungal concentration of the drug is
361 achievable through periodic drops alone suggest this class of compounds can be fruther
362 optimized for ophthalmic use. Ongoing studies are aimed at elucidating the fungal physiological
363 response to the drug as well as methods to optimize delivery to increase the effective
364 concentration within the cornea.
365 We note that 4μ8C treatment did not alter corneal clarity or tissue thickness in uninfected
366 controls, suggesting the compound does not promote corneal inflammation or edema, the latter
367 of which can arise upon corneal endothelial dysfunction (28,29). We do observe, however, a
368 transient block of corneal re-epithelialization, which is consistent with the known anti-proliferative
369 effects of the compound (23,26). While at face value this represents a unwanted side-effect of the
370 drug, we typically do not observe corneal re-peithelization of activity infected corneas in our model
371 (9,19). In the clinical setting, we further note that a transient impact of the drug on epithelial
372 integrity may actually be clinically useful. Indeed, a major barrier to corneal penetration of topically
373 applied drugs is the epithelium and, consequently, this cellular layer is often debrided by clinicians
374 to improve drug delivery. In the setting of fungal keratitis, for example, corneal debridement
375 precedes the topical application of photosensitizers in photodynamic therapy (30,31). Thus, the
376 antiproliferative effect of the 4μ8C may actually facilitate drug penetration in ulcerated eyes and
377 promote its antifungal efficacy. Another important consideration is that 4μ8C also inhibits TGFβ-
378 driven fibroblast activation and liver fribrosis *in vivo* (27,32). As myofribroblast transformation and
379 corneal scarring are important long-term complications of FK (33–35), i.e., even if corneal
380 sterilization is acheived, we further reason that 4μ8C treatment alone or in conjuction with other
381 antifungals may improve visual outcomes post-infection. One final and potential impact of 4μ8C
382 on host physiology not addressed in this study is on the ocular inflammatory response. Recently,
383 Kumar et al. demonsrated that intravitreal injection of 4μ8C blocks the host pro-inflammatory
384 response in a murine model of *Staphylococcus* endophthalmitis due to an Ire1-dependent
385 activation of NK-kB signaling downstream of the Toll-like receptor 2 (38). The consequence of
386 4μ8C treatment in those experiments was uncontrolled bacterial growth and worsened disease
387 outcomes. However, as fungi are also impacted by the compound, we suspect that 4μ8C may
388 serve as a dual-edged sword that mitigates corneal damage caused by both the fungus and the
389 host response (immunopathogenesis). We did not observe an obvious reduction in inflammation
390 upon treatment with 0.5 mM 4μ8C, but *in vitro* studies will be required to more directly assess the
391 impact of the compound on the pro-inflammatory response of corneal cells to fungal antigen.
392 In summary, the current study serves as an important proof-of-principle for the
393 development of UPR-targeting antifungals. It also highlights the relevance of the corneal model
394 for antifungal development more generally, as it allows for the longitudinal tracking of host toxicity
395 and disease development before transitioning into visceral organ or systemic models of infection.
396 Regarding FK, it is important to note that patients typically present to the clinic after the
397 development of clinical signs of disease, including corneal haze or corneal ulcer formation. Thus,
398 while we have demonstrated that 4μ8C can effectively kill *A. fumigatus* on the ocular surface and
399 block disease establishment in our model, future studies will need to investigate treatment efficacy
400 at later time points post-inoculation. We will further address the antifungal properties, both *in vitro*

9

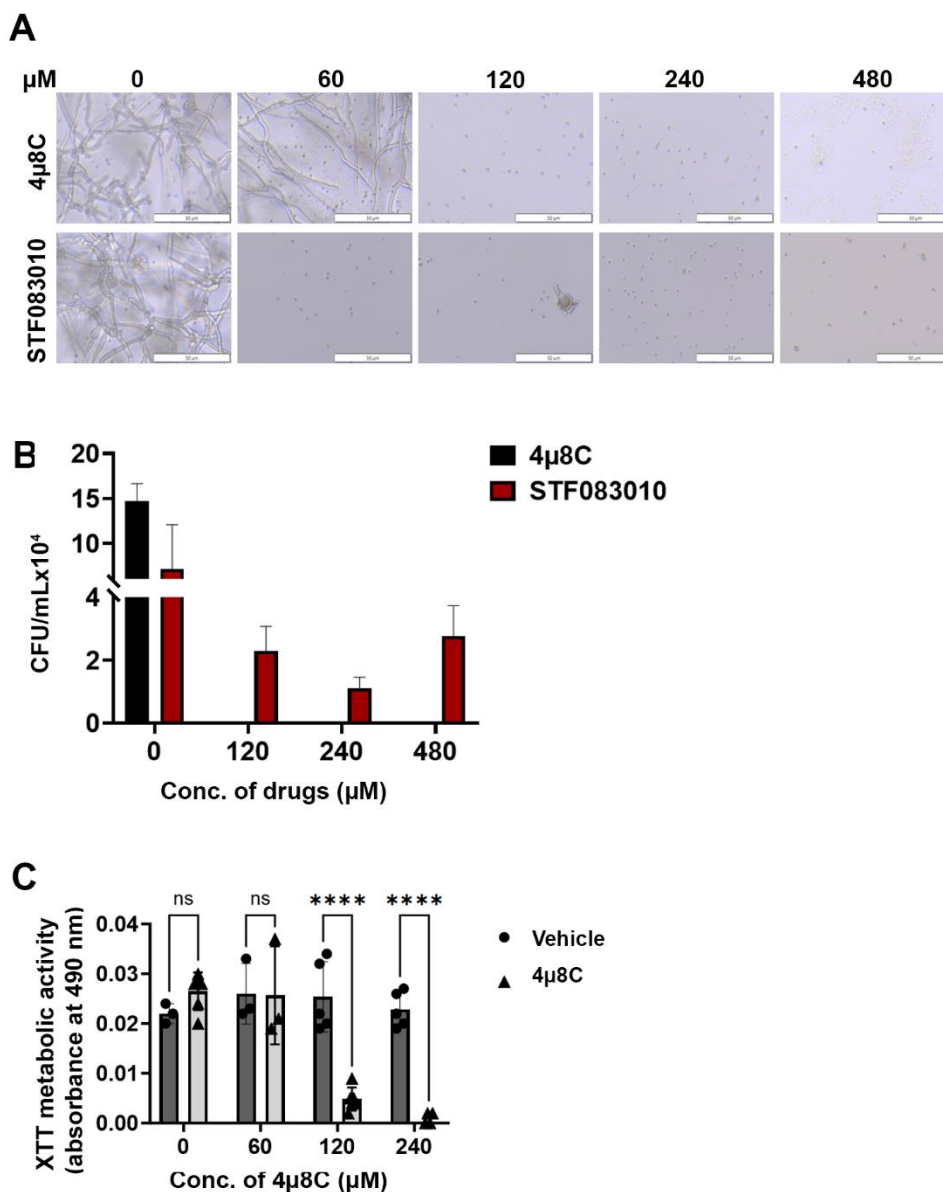401 and *in vivo*, against other FK-relevant fungi, including *Candida albicans* and various *Fusarium*
402 species.
403

References

1. Thomas PA. Fungal infections of the cornea. Eye. 2003;17(8):852–62.

2. Cabrera-Aguas M, Khoo P, Watson SL. Infectious keratitis: A review. Clin Exp Ophthalmol. 2022;50(5):543–62.

3. Atta S, Perera C, Kowalski RP, Jhanji V. Fungal Keratitis: Clinical Features, Risk Factors, Treatment, and Outcomes. J Fungi. 2022;8(9).

4. Acharya Y, Acharya B, Karki P. Fungal keratitis: study of increasing trend and common determinants. Nepal J Epidemiol. 2017; 7 (2): 685–93.

5. Lalitha P, Prajna NV, Kabra A, Mahadevan K SM. Risk factors for treatment outcome in fungal keratitis. Opthalmology. 2006;113(4):526–30.

6. Ansari Z, Miller D, Galor A. Current thoughts in fungal keratitis: Diagnosis and treatment. Curr Fungal Infect Rep. 2013;7(3):209–18.

7. Richie DL, Hartl L, Aimanianda V, Winters MS, Fuller KK, Miley MD, et al. A role for the unfolded protein response (UPR) in virulence and antifungal susceptibility in Aspergillus fumigatus. PLoS Pathog. 2009;5(1).

8. Feng X, Krishnan K, Richie DL, Aimanianda V, Hartl L, Grahl N, et al. Haca-independent functions of the ER stress sensor irea synergize with the canonical UPR to influence virulence traits in Aspergillus fumigatus. PLoS Pathog. 2011;7(10).

9. Kamath MM, Lightfoot JD, Adams EM, Kiser RM, Wells BL, Fuller KK. The Aspergillus fumigatus UPR is variably activated across nutrient and host environments and is critical for the establishment of corneal infection [Internet]. Vol. 19, PLoS Pathogens. 2023. 1–32 p. Available from: http://dx.doi.org/10.1371/journal.ppat.1011435

10. Ron D, Walter P. Signal integration in the endoplasmic reticulum unfolded protein response. Nat Rev Mol cell Biol. 2007;8(7):519–29.

11. Zhang L, Zhang C, Wang A. Divergence and conservation of the major UPR branch IRE1-bZIP signaling pathway across eukaryotes. Sci Rep. 2016;6(1):27362.

12. Verchot J, Pajerowska-Mukhtar KM. UPR signaling at the nexus of plant viral, bacterial, and fungal defenses. Curr Opin Virol. 2021;47:9–17.
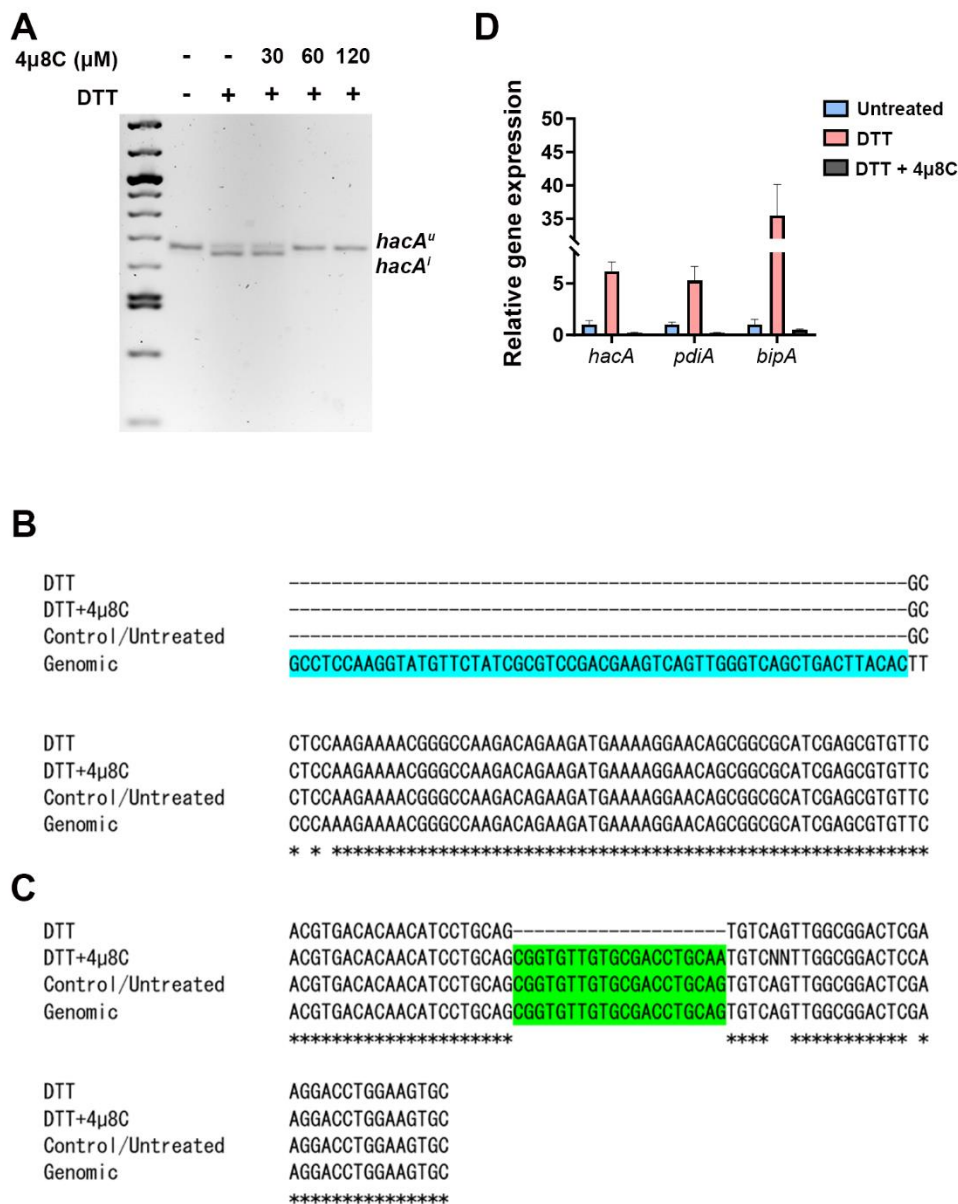
443 13. Sircaik S, Andes DR, Panwar SL, Román E, Gow NAR, Bapat P, et al. The protein kinase
444   Ire1 impacts pathogenicity of Candida albicans by regulating homeostatic adaptation to
445   endoplasmic reticulum stress. 2021;(August 2020):1–19.

446 14. Ishiwata-Kimata Y, Kimata Y. Fundamental and Applicative Aspects of the Unfolded
447   Protein Response in Yeasts. J Fungi. 2023;9(10):989.

448 15. Richie DL, Feng X, Hartl L, Aimanianda V, Krishnan K, Powers-Fletcher M V., et al. The
449   virulence of the opportunistic fungal pathogen aspergillus fumigatus requires cooperation
450   between the endoplasmic reticulum-associated degradation pathway (ERAD) and the
451   unfolded protein response (UPR). Virulence. 2011;2(1):12–21.

452 16. Cox JS, Walter P. A Novel Mechanism for Regulating Activity of a Transcription Factor That
453   Controls the Unfolded Protein Response. 1996;87:391–404.

454 17. Sidrauski C, Walter P. The transmembrane kinase Ire1p is a site-specific endonuclease
455   that initiates mRNA splicing in the unfolded protein response. Cell. 1997;90(6):1031–9.

456 18. Guirao-Abad JP, Weichert AM, Albee A, Deck K, Askew DS. A Human IRE1 Inhibitor
457   Blocks the Unfolded Protein Response in the Pathogenic Fungus Aspergillus fumigatus
458   and Suggests Noncanonical Functions within the Pathway. mSphere. 2020;5(5):1–13.

459 19. Lightfoot JD, Adams EM, Kamath MM, Wells BL, Fuller KK. Aspergillus fumigatus hypoxia
460   adaptation is critical for the establishment of fungal keratitis. Invest Ophthalmol Vis Sci.
461   2024;65(4):31.

462 20. Cove DJ. The induction and repression of nitrate reductase in the fungus Aspergillus
463   nidulans. Biochim Biophys Acta [Internet]. 1966;113(1):51–6. Available from:
464   http://dx.doi.org/10.1016/S0926-6593(66)80120-0

465 21. Pierce CG, Uppuluri P, Tristan AR, Wormley Jr FL, Mowat E, Ramage G, et al. A simple
466   and reproducible 96-well plate-based method for the formation of fungal biofilms and its
467   application to antifungal susceptibility testing. Nat Protoc. 2008;3(9):1494–500.

468 22. Zhao J, Wu XY, Yu FSX. Activation of Toll-like receptors 2 and 4 in Aspergillus fumigatus
469   keratitis. Innate Immun. 2009;15(3):155–68.

470 23. Cross BCS, Bond PJ, Sadowski PG, Jha BK, Zak J, Goodman JM, et al. The molecular
471   basis for selective inhibition of unconventional mRNA splicing by an IRE1-binding small
472   molecule. Proc Natl Acad Sci. 2012;109(15):E869–78.

473 24. Kim JH, Cheng LW, Chan KL, Tam CC, Mahoney N, Friedman M, et al. Antifungal drug
474   repurposing. Antibiotics. 2020;9(11):812.

475 25. Qiu Q, Zheng Z, Chang L, Zhao Y, Tan C, Dandekar A, et al. Toll-like receptor-mediated
476   IRE1α activation as a therapeutic target for inflammatory arthritis. EMBO J.
477   2013;32(18):2477–90.

478 26. Stewart C, Estrada A, Kim P, Wang D, Wei Y, Gentile C, et al. Regulation of IRE1α by the
479   small molecule inhibitor 4μ8c in hepatoma cells. Cell Pathol. 2017;4(1):1–10.

480 27. Pavlović N, Calitz C, Thanapirom K, Mazza G, Rombouts K, Gerwins P, et al. Inhibiting
481   IRE1α-endonuclease activity decreases tumor burden in a mouse model for hepatocellular
482   carcinoma. Elife. 2020;9:e55865.

483 28. Feizi S. Corneal endothelial cell dysfunction: etiologies and management. 2018. p. 10:

484   2515841418815802.

485   29.   Price MO, Mehta JS, Jurkunas U V, Price Jr FW. Corneal endothelial dysfunction: Evolving
486   understanding and treatment options. Prog Retin Eye Res. 2021;82:100904.

487   30.   Li J, Li Z, Liang Z, Han L, Feng H, He S, et al. Fabrication of a drug delivery system that
488   enhances antifungal drug corneal penetration. Drug Deliv. 2018;25(1):938–49.

489   31.   Szentmáry N, Goebels S, Bischoff M, Seitz B. Photodynamic therapy for infectious keratitis.
490   Der Ophthalmol. 2012;109:165–70.

491   32.   Heindryckx F, Binet F, Ponticos M, Rombouts K, Lau J, Kreuger J, et al. Endoplasmic
492   reticulum stress enhances fibrosis through IRE 1α-mediated degradation of miR-150 and
493   XBP-1 splicing. EMBO Mol Med. 2016;8(7):729–44.

494   33.   Zhou Y, Chen Y, Wang S, Qin F, Wang L. MSCs helped reduce scarring in the cornea after
495   fungal infection when combined with anti-fungal treatment. BMC Ophthalmol.
496   2019;19(1):1–11.

497   34.   Menda SA, Das M, Panigrahi A, Prajna NV, Acharya NR, Lietman TM, et al. Association of
498   postfungal keratitis corneal scar features with visual acuity. JAMA Ophthalmol.
499   2020;138(2):113–8.

500   35.   Hazlett L, Suvas S, McClellan S, Ekanayaka S. Challenges of corneal infections. Expert
501   Rev Ophthalmol. 2016;11(4):285–97.

Figure 1: 4µ8C displays antifungal activity against A. fumigatus Af293 conidia and hyphae *in vitr*o. (A) Conidia of *A. fumigatus* Af293 were inoculated into GMM broth containing the indicated concentration of 4µ8C or STF-083010 and incubated for 72 h at 35 °C. Images represent a consistent result observed across three independent experiments. (B) 100 µL aliquots were taken from wells of microbroth dilution assay, like the one shown in panel A, and spread onto YPD plates. Colonies were enumerated following 24 h incubation at 35 °C. The data reflect the mean CFU counts from triplicate wells of a single microbroth experiment. (C) Af293 biofilms generated in GMM were treated with vehicle (DMSO) or the indicated concentration of 4µ8C for 2 h at 35 °C. Metabolic activity was measured by XTT reduction. The data reflect the mean 490 nm absorbance (± SD) of triplicate wells in single experiment and groups were compared by Two-way ANOVA **** <0.001. Similar results were recapitulated across three independent experiments.

13

A

4µ8C (µM)   -   -   30 60 120
DTT   -   +   +   +   +

hacA^u
hacA^l

D

B

```
DTT                -----------------------------------------------------GC
DTT+4µ8C           -----------------------------------------------------GC
Control/Untreated  -----------------------------------------------------GC
Genomic            GCCTCCAAGGTATGTTCTATCGCGTCCGACGAAGTCAGTTGGGTCAGCTGACTTACACTT

DTT                CTCCAAGAAAACGGGCCAAGACAGAAGATGAAAAGGAACAGCGGCGCATCGAGCGTGTTC
DTT+4µ8C           CTCCAAGAAAACGGGCCAAGACAGAAGATGAAAAGGAACAGCGGCGCATCGAGCGTGTTC
Control/Untreated  CTCCAAGAAAACGGGCCAAGACAGAAGATGAAAAGGAACAGCGGCGCATCGAGCGTGTTC
Genomic            CCCAAAGAAAACGGGCCAAGACAGAAGATGAAAAGGAACAGCGGCGCATCGAGCGTGTTC
                   *  *  ***********************************************************
```

C

```
DTT                ACGTGACACAACATCCTGCAG--------------------TGTCAGTTGGCGGACTCGA
DTT+4µ8C           ACGTGACACAACATCCTGCAGCGGTGTTGTGCGACCTGCAATGTCNNTTGGCGGACTCCA
Control/Untreated  ACGTGACACAACATCCTGCAGCGGTGTTGTGCGACCTGCAGTGTCAGTTGGCGGACTCGA
Genomic            ACGTGACACAACATCCTGCAGCGGTGTTGTGCGACCTGCAGTGTCAGTTGGCGGACTCGA
                   ********************               ****  ********** *

DTT                AGGACCTGGAAGTGC
DTT+4µ8C           AGGACCTGGAAGTGC
Control/Untreated  AGGACCTGGAAGTGC
Genomic            AGGACCTGGAAGTGC
                   ***************
```

518
519
520 **Figure 2: The antifungal activity of 4µ8C corresponds to an inhibition of Ire1 activity in**
521 **Af293.** Af293 biofilms generated overnight in GMM were pre-treated with 4µ8C or DMSO for 2 h
522 and subsequently spiked with 10 mM DTT and incubated for an additional 2 h prior to total RNA
523 isolation and cDNA synthesis. (A) The full-length *hacA* message was amplified and the *hacA^u*
524 (uninduced: 665 bp) and *hacA^i* (induced: 645 bp) products were resolved by gel electrophoresis.
525 The end point *hacA* PCR products were sequenced and a CLUSTAL multiple sequence alignment
526 was performed in the regions spanning the canonical/spliceosome intron highlighted in blue (B)
527 and the IreA-targeted non-canonical intron highlighted in green (C). (D) qPCR was performed on
528 total *hacA* as well as two chaperone encoding genes, *bipA* and *pdiA*. The qPCR data reflect the
529 mean $2^{\Delta\Delta Ct}$ calculations for triplicate fungal samples from a single experiment. Similar results were
530 observed in an independent experiment.
531
532

14

533
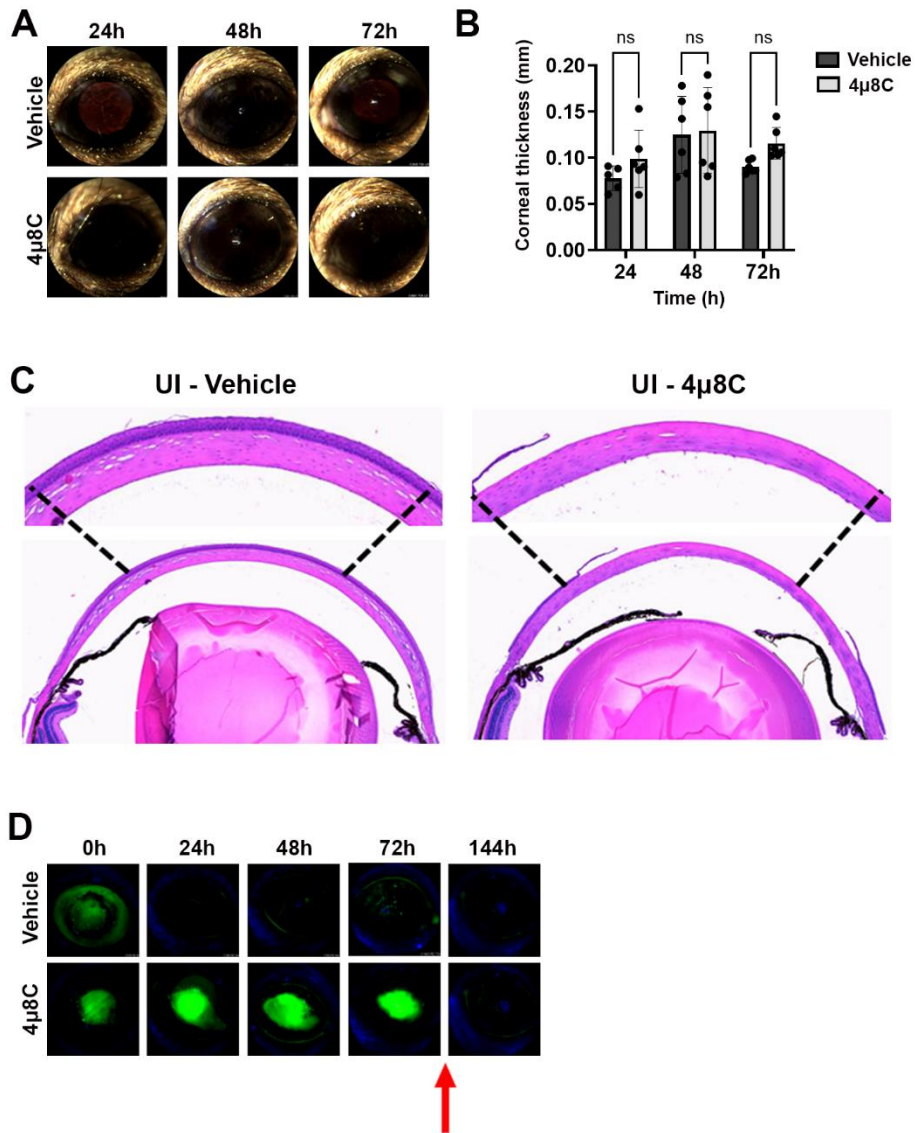
534
535
536
537 **Figure 3: High dose 4μ8C treatment does not impact corneal clarity but does transiently**
538 **inhibit re-epithelialization.** Sham-inoculated (UI) corneas were treated with topical drops of 2.5
539 mM 4μ8C or vehicle (DMSO), once on the day on ulceration (4 h p.i.), three times (4 h apart) the
540 following three days. (A) Representative external images taken each day post-ulceration. (B)
541 Corneal thickness was measured daily based on OCT images (n = 6/group). Groups were
542 compared by Two-way ANOVA; (C) Representative histological (H&E) sections taken at 72 h post-
543 ulceration; 400X magnification. (D) In a separate experiment, ulcerated eyes were treated as
544 described above and on each day the penetration of fluorescein was imaged by a fluorescent slit-
545 lamp (Micron IV). The red arrow indicates that the treatment was stopped, and the eyes were
546 monitored for an additional three days.
547
548
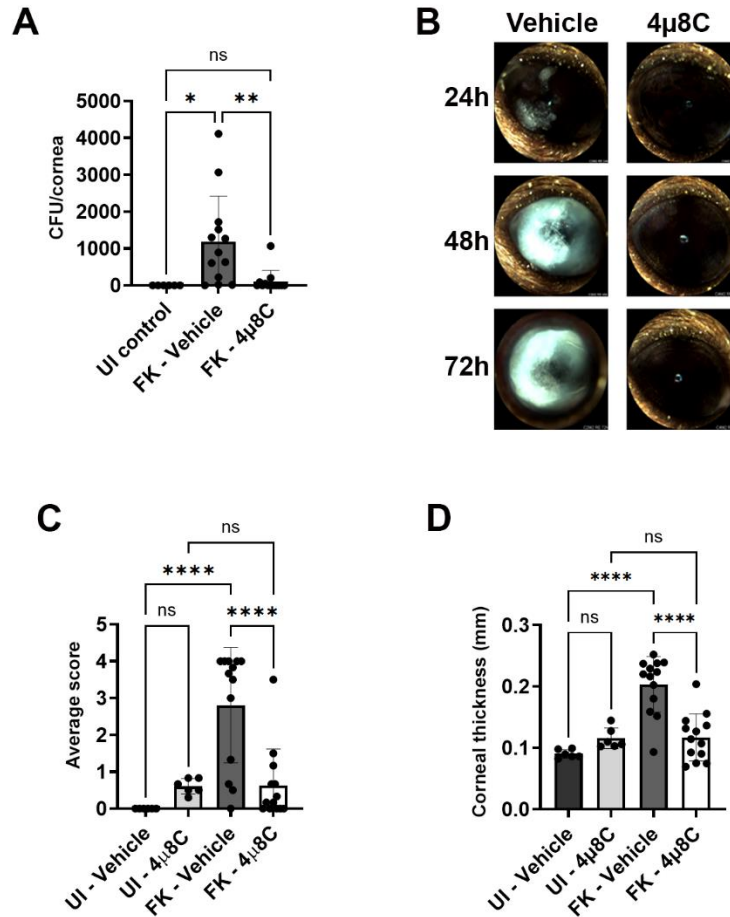
Figure 4: Topical treatment with 4µ8C blocks fungal growth and disease establishment in a murine model of FK. Sham (UI) or Af293-inoculated (FK) corneas were treated with 2.5 mM 4µ8C or vehicle for up to 72 h p.i. as described in the figure 3 legend. The data in all panels reflect a pool of two independent experiments (n=6 per UI group; n=13 per FK group). (A) Fungal burden at 72 h p.i.. Groups were compared by Ordinary one-way ANOVA p-value ** 0.0061, * 0.0173; (B) Representative external images taken each day p.i. (C) Average clinical scores at 72 h p.i.; Groups were compared by Ordinary one-way ANOVA p-value **** <0.0001; (D) Corneal thickness measured at 72 h p.i.. Groups were compared by Ordinary one-way ANOVA p-value **** <0.0001
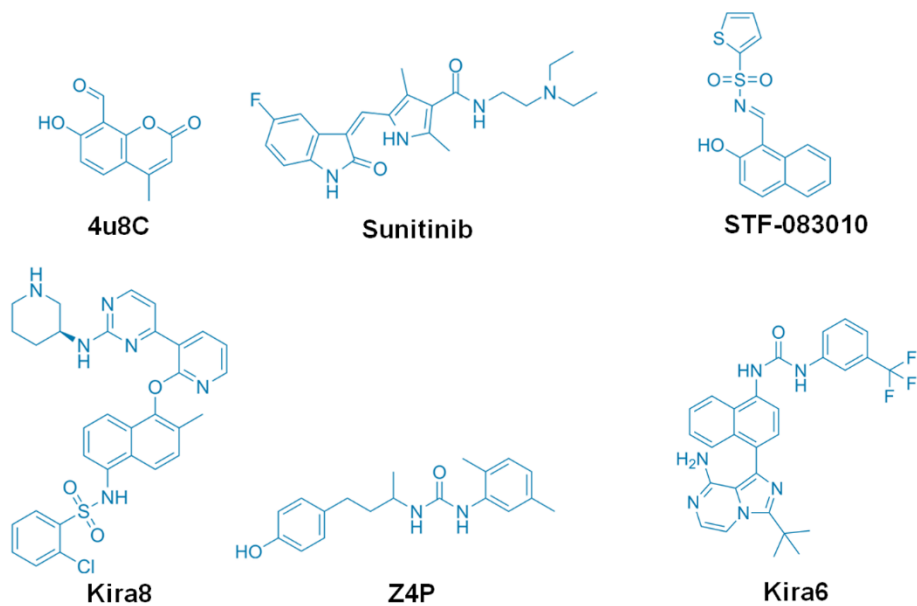
Figure S1: Chemical structure of the drugs screened in this study.
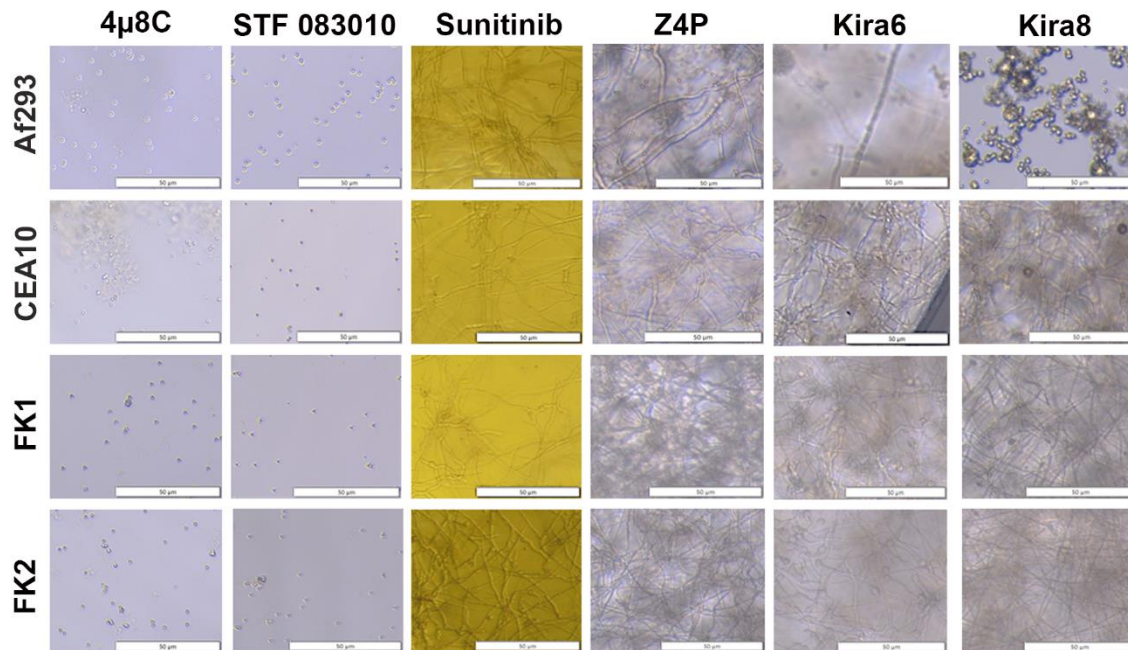
567
568
Figure S2: The Ire1 kinase domain inhibitors do not display antifungal activity *in vitro*.
Conidia of the *A. fumigatus* isolates were inoculated into GMM broth containing the 480 µM of the indicated drug and incubated for 72 h at 35 °C. Images represent a consistent result observed across three independent experiments.
573
574

18
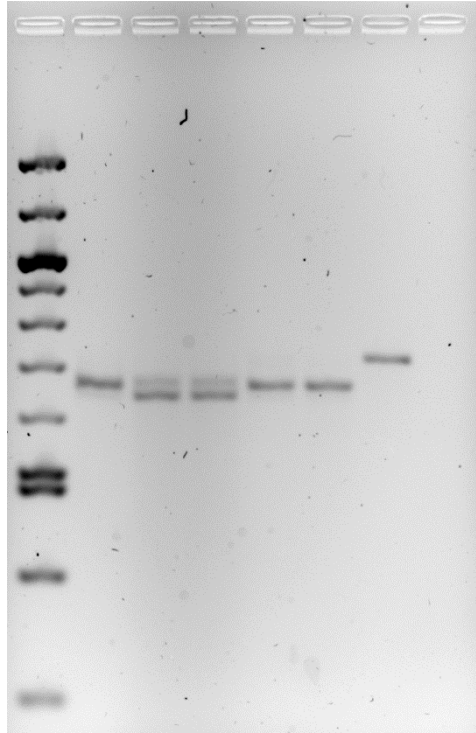
575
576
577 **Figure S3: Unaltered agarose gel image corresponding to Figure 2.** The original/raw ethidium
578 bromide gel image captured from the Alliance Q9 Advanced Chemidoc (Uvitec) imaging platform.
579 The image is unaltered in Figure 2A beyond the cropping of the rightmost two lanes, which
580 correspond to the Af293 gDNA and no-template control amplicons, respectively.
581
582

583
584
585
586
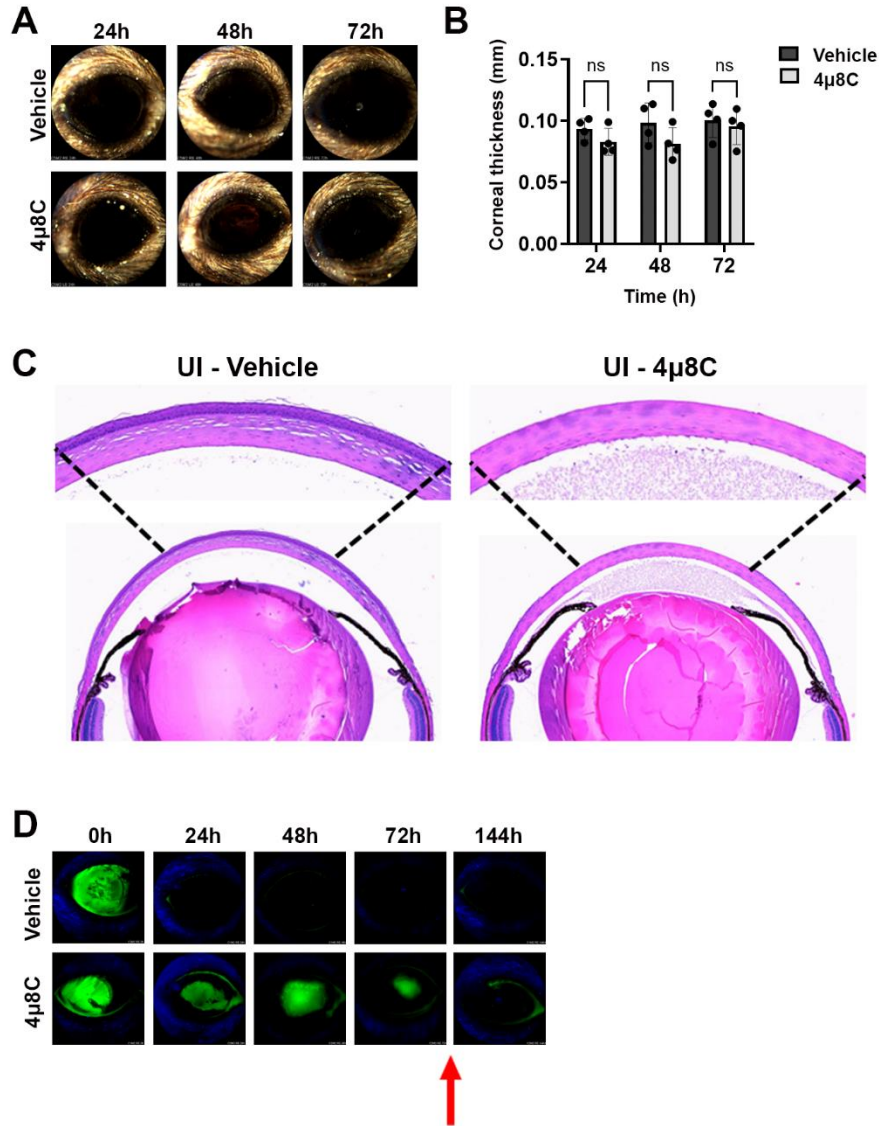
Figure S4: 0.5 mM 4µ8C treatment does not impact corneal clarity but does transiently inhibit re-epithelialization. Sham-inoculated (UI) corneas were treated with topical drops of 0.5 mM 4µ8C or vehicle (DMSO) three times per day (4 h apart) starting on day after ulceration. (A) Representative external images taken each day post-ulceration. (B) Corneal thickness was measured daily based on OCT images. Groups were compared by Two-way ANOVA; (C) Representative histological (H&E) sections taken at 72 h post-ulceration; 400X magnification. (D) In a separate experiment, ulcerated eyes were treated as described above and on each day the penetration of fluorescein was imaged by a fluorescent slit-lamp (Micron IV). The red arrow indicates that the treatment was stopped, and the eyes were monitored for an additional three days.

597
598

20
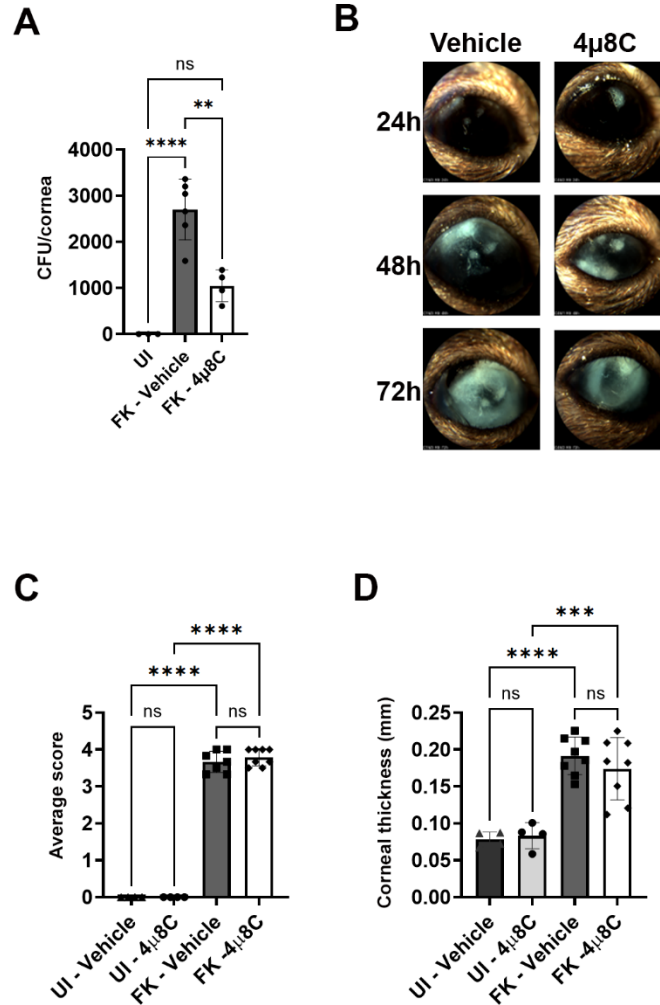
599
600
601

Figure S5: Treatment with 0.5 mM 4µ8C reduces fungal burden but has no significant impact on clinical disease severity. Af293-inoculated (FK) corneas were treated with topical drops of 0.5 mM 4µ8C or vehicle (DMSO) 3X per day starting on day after ulceration and as described in the methods. The data reflect results from a single experiment (n=4 per UI group; n=8 per FK group). (A) Fungal burden at 72 h p.i.. Groups were compared by Ordinary one-way ANOVA p-value **** <0.0001, ** 0.0012 (n=3, UI; n=6, FK-vehicle; n=4, FK-4µ8C); (B) Representative micron images over the course of the infection. (C) Average clinical scores at 72 h p.i. Groups were compared by Ordinary one-way ANOVA, p-value **** <0.0001; (C) Corneal thickness measurements at 72 h p.i.. Groups were compared by Ordinary one-way ANOVA p-value **** <0.0001, *** 0.0003.

21